Digital Signal Processing 24 (2014) 34–41

Contents lists available at ScienceDirect

Digital Signal Processing

www.elsevier.com/locate/dsp

Two-dimensional angle estimation for monostatic MIMO arbitrary array with velocity receive sensors and unknown locations

Jianfeng Li *, Xiaofei Zhang

College of Electronic and Information Engineering, Nanjing University of Aeronautics and Astronautics, Nanjing 210016, China

ARTICLE INFO

Article history:
Available online 30 August 2013

Keywords:
Angle estimation
Multi-input multi-output array
Velocity sensor
Rotational invariance technique

ABSTRACT

In this paper, the problem of two-dimensional angle estimation for monostatic multi-input multi-output (MIMO) array is studied, and an algorithm based on the usage of velocity receive sensors is proposed. The algorithm applies the estimation method of signal parameters via rotational invariance technique (ESPRIT) algorithm to obtain automatically paired two-dimensional angle estimation. By utilizing the relationship within the outputs of velocity sensors, the rotational invariance property of ESPRIT does not depend on the array geometry any more. Hence, the proposed algorithm can provide two-dimensional DOA estimation for the MIMO array without the knowledge of sensor locations in the array. The algorithm requires no peak searches, so it has low complexity. Furthermore, it has better angle estimation performance than propagator method using the same sensor configuration. Error analysis and Cramér–Rao bound (CRB) of angle estimation in MIMO radar are derived. Simulation results verify the usefulness of the algorithm.

1. Introduction

Multi-input multi-output (MIMO) array systems have been used in radar and sonar systems for target location and detection to overcome fading effect, enhance spatial resolution and improve target detection performance [1–4]. Direction of departure (DOD) and direction of arrival (DOA) estimation for MIMO array is an important issue and has been investigated recently. Maximal likelihood method [5] has been used for angle estimation for MIMO array, but it requires an exhaustive multi-dimensional peak searches, which renders high computational complexity. Capon algorithm [6] and multiple signal classification (MUSIC) algorithms [7–9] can all work well for high-resolution angle estimation with arbitrary array geometry, but the peak searches with high complexity are also needed. Estimation of signal parameters via rotational invariance technique (ESPRIT) algorithm [10], which exploits the invariance property in the array, was applied for direction estimation in MIMO radar systems [11–13]. Unitary ESPRIT [14] transforms the complex computations in ESPRIT into real-valued ones to reduce the complexity. Ref. [15] proposed a low-complexity ESPRIT-based method for angle estimation in monostatic MIMO radar and the reduced-dimension transformation can obtain signal to noise ratio (SNR) gain. Ref. [16] proposed an ESPRIT-like algorithm which can work well for coherent DOA estimation. Propagator method (PM) was proposed in [17] and was applied for angle estimation in MIMO array [18,19]. PM utilizes the relationship within the receive data to calculate a propagator matrix and then construct the signal subspace or noise subspace without the eigen-value decomposition (EVD). Hence, it has lower complexity than ESPRIT or MUSIC. Parallel factor analysis (PARAFAC) algorithm has also been used for localization of multiple targets in a MIMO radar system based on the trilinear decomposition [20]. MUSIC and PARAFAC can work well for arbitrary array geometry, but the peak searching and iteration will lead to a high complexity. Ref. [21] proposed a method based on the signal subspace to deal with arbitrary arrays without peak searching and iteration, but the knowledge of sensor locations is needed and the maximum number of detectable targets is reduced.

The usage of velocity sensor arrays is a key technology of sonar and radar systems [22,23]. Compared to scalar sensor array, velocity sensor array has more degrees of freedom. These additional degrees of freedom can enhance spatial resolution, strengthen parameter identifiability and improve target detection performance. By combining the velocity sensor and pressure sensor, an ESPRIT-based method was proposed in [23] to achieve the underwater angle estimation without the knowledge of sensor locations, but an additional pairing was needed. Ref. [24] proposed a successive MUSIC algorithm for angle estimation with velocity receive sensors in MIMO array, and it avoided the two-dimensional peak searching in two-dimensional (2D) MUSIC. Though successive MUSIC algorithm can be used for arbitrary array, it requires a priori knowledge of the array geometry. Furthermore, it requires peak searching, which relies on a heavy computational load.

* Corresponding author.
E-mail address: lijianfengtin@126.com (J. Li).

1051-2004/$ – see front matter
http://dx.doi.org/10.1016/j.dsp.2013.08.005

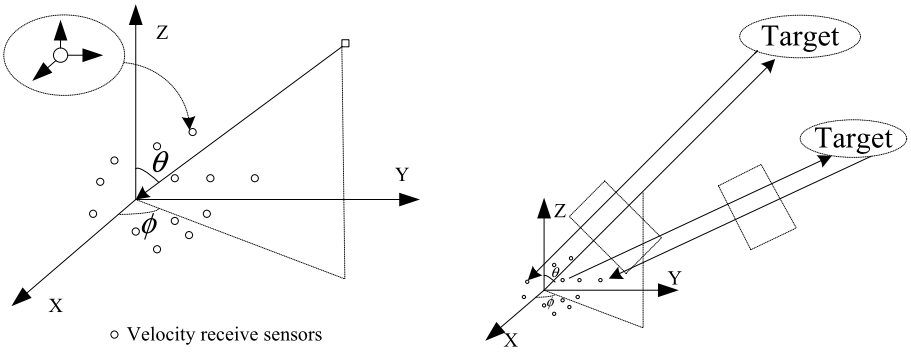

(a).Sensor array structure. (b). Framework of MIMO array system

Fig. 1. MIMO array with velocity receive sensors.

In this paper, we consider the problem of two-dimensional angle estimation in monostatic MIMO array, which is configured with multiple transmit sensors and velocity receive sensors. The proposed algorithm applies ESPRIT algorithm to obtain automatically paired two-dimensional angle estimation. As the output of the velocity sensor is a vector along different axes, the rotational invariance can be acquired regardless of the array geometry. Hence, the proposed algorithm can provide two-dimensional DOA estimation for the MIMO array without the knowledge of sensor locations in the array. Furthermore, the proposed algorithm requires no peak searches and has better angle estimation performance than PM using the same sensor configuration.

The remainder of this paper is structured as follows. Section 2 develops the data model of Monostatic MIMO radar, and Section 3 proposes the DOA estimation algorithm. Section 4 presents the angle estimation error analysis, Section 5 derives Cramér–Rao bound (CRB) of angle estimation and Section 6 gives the complexity analysis. In Section 7, simulation results are presented, while our conclusions are shown in Section 8.

Notation. $(.)^T$, $(.)^H$, $(.)^{-1}$ and $(.)^+$ denote transpose, conjugate transpose, matrix inverse and matrix pseudo-inverse, respectively. diag($\mathbf{v}$) stands for diagonal matrix whose diagonal is a vector $\mathbf{v}$. $\mathbf{I}_P$ is an identity matrix with the dimension $P \times P$. $\otimes$, $\circ$ and $\odot$ are the Kronecker product, Khatri–Rao product and Hadamard product, respectively. $\mathbf{0}_I$ is an all-zero vector with the length I. tr$(\cdot)$ is to get the trace of a matrix. $\Delta\boldsymbol{\Psi}$ means the estimation error of $\boldsymbol{\Psi}$.

2. Data model

Consider a monostatic MIMO array which is configured with M transmit sensors and N velocity receive sensors. Assume that the sensors of transmit array and receive array are placed at arbitrary unknown three-dimensional positions. Each of the N receive sensors consists of three identical but orthogonally oriented velocity sensors, aligning along the X-axis, the Y-axis and Z-axis, respectively (see Fig. 1(a)). The velocity sensor itself can determine the coordinate when the reference point location is determined. Define the location of the mth sensor in transmit array as (x_{tm}, y_{tm}, z_{tm}) and the location of the nth sensor in receive array as (x_{rn}, y_{rn}, z_{rn}). The transmit sensors send mutually orthogonal signals, which will be reflected by the targets and received by the velocity receive sensors. Assume that there are K non-coherent targets, with (θ_k, ϕ_k) being the elevation and azimuth of the kth target with respect to the reference point in Fig. 1(a).

Fig. 1(b) shows the framework of MIMO array system. The targets are assumed to be far-away enough, so the arrived reflect signals from one target can be regarded as a plane wave. According to [24], the output of the matched filters for the velocity receive sensors contains three parts (the data along the X-axis, the data along the Y-axis and the data along the Z-axis), which can be expressed as

$$\mathbf{x}(t) = \begin{bmatrix} \mathbf{x}_x(t) \\ \mathbf{x}_y(t) \\ \mathbf{x}_z(t) \end{bmatrix} \tag{1a}$$

$$\begin{aligned}\mathbf{x}_x(t) &= \big[\sin\theta_1\cos\phi_1\mathbf{a}_r(\theta_1,\phi_1)\otimes\mathbf{a}_t(\theta_1,\phi_1),\ldots,\\ &\quad \sin\theta_K\cos\phi_K\mathbf{a}_r(\theta_K,\phi_K)\otimes\mathbf{a}_t(\theta_K,\phi_K)\big]\mathbf{b}(t)+\mathbf{n}_x(t)\\ &= \mathbf{A}\boldsymbol{\Phi}_x\mathbf{b}(t)+\mathbf{n}_x(t)\end{aligned} \tag{1b}$$

$$\begin{aligned}\mathbf{x}_y(t) &= \big[\sin\theta_1\sin\phi_1\mathbf{a}_r(\theta_1,\phi_1)\otimes\mathbf{a}_t(\theta_1,\phi_1),\ldots,\\ &\quad \sin\theta_K\sin\phi_K\mathbf{a}_r(\theta_K,\phi_K)\otimes\mathbf{a}_t(\theta_K,\phi_K)\big]\mathbf{b}(t)+\mathbf{n}_y(t)\\ &= \mathbf{A}\boldsymbol{\Phi}_y\mathbf{b}(t)+\mathbf{n}_y(t)\end{aligned} \tag{1c}$$

$$\begin{aligned}\mathbf{x}_z(t) &= \big[\cos\theta_1\mathbf{a}_r(\theta_1,\phi_1)\otimes\mathbf{a}_t(\theta_1,\phi_1),\ldots,\\ &\quad \cos\theta_K\mathbf{a}_r(\theta_K,\phi_K)\otimes\mathbf{a}_t(\theta_K,\phi_K)\big]\mathbf{b}(t)+\mathbf{n}_z(t)\\ &= \mathbf{A}\boldsymbol{\Phi}_z\mathbf{b}(t)+\mathbf{n}_z(t)\end{aligned} \tag{1d}$$

where $\mathbf{a}_r(\theta_k,\phi_k)$ and $\mathbf{a}_t(\theta_k,\phi_k)$ are the receive steering vector and the transmit steering vector of the kth target, respectively (see Eq. (2)). $\mathbf{A} = [\mathbf{a}_r(\theta_1,\phi_1)\otimes\mathbf{a}_t(\theta_1,\phi_1),\ldots,\mathbf{a}_r(\theta_K,\phi_K)\otimes\mathbf{a}_t(\theta_K,\phi_K)]$, and $\boldsymbol{\Phi}_x$, $\boldsymbol{\Phi}_y$ and $\boldsymbol{\Phi}_z$ are diagonal matrices (see Eq. (3)). $\mathbf{b}(t) = [b_1(t), b_2(t),\ldots,b_K(t)]^T \in \mathbb{C}^{K\times 1}$, and $b_k(t) = \beta_k e^{j2\pi f_k t}$ with f_k and β_k being the Doppler frequency and amplitude, respectively. $\mathbf{n}_x(t)$, $\mathbf{n}_y(t)$ and $\mathbf{n}_z(t)$ are the received additive white Gaussian noise vectors with zero mean and the covariance matrix $\sigma^2\mathbf{I}_{MN}$.

$$\begin{aligned}\mathbf{a}_r(\theta_k,\phi_k) &= \big[\exp\big(-j2\pi(x_{r1}\sin\theta_k\cos\phi_k+y_{r1}\sin\theta_k\sin\phi_k\\ &\quad +z_{r1}\cos\theta_k)/\lambda\big),\ldots,\exp\big(-j2\pi(x_{rN}\sin\theta_k\cos\phi_k\\ &\quad +y_{rN}\sin\theta_k\sin\phi_k+z_{rN}\cos\theta_k)/\lambda\big)\big]^T\end{aligned} \tag{2a}$$

$$\begin{aligned}\mathbf{a}_t(\theta_k,\phi_k) &= \big[\exp\big(-j2\pi(x_{t1}\sin\theta_k\cos\phi_k+y_{t1}\sin\theta_k\sin\phi_k\\ &\quad +z_{t1}\cos\theta_k)/\lambda\big),\ldots,\exp\big(-j2\pi(x_{tM}\sin\theta_k\cos\phi_k\\ &\quad +y_{tM}\sin\theta_k\sin\phi_k+z_{tM}\cos\theta_k)/\lambda\big)\big]^T\end{aligned} \tag{2b}$$

$$\boldsymbol{\Phi}_x = \mathrm{diag}(\sin\theta_1\cos\phi_1,\ldots,\sin\theta_K\cos\phi_K) \tag{3a}$$

$$\boldsymbol{\Phi}_y = \mathrm{diag}(\sin\theta_1\sin\phi_1,\ldots,\sin\theta_K\sin\phi_K) \tag{3b}$$

$$\boldsymbol{\Phi}_z = \mathrm{diag}(\cos\theta_1,\ldots,\cos\theta_K) \tag{3c}$$

3. The proposed angle estimation algorithm

For the signal model in (1), the covariance matrix $\hat{\mathbf{R}}_x$ can be estimated with J snapshots by $\hat{\mathbf{R}}_x = (1/J)\sum_{t=1}^{J}\mathbf{x}(t)\mathbf{x}^H(t)$. Perform eigen-value decomposition; $\hat{\mathbf{R}}_x$ is denoted by

$$\hat{\mathbf{R}}_x = \hat{\mathbf{E}}_s\hat{\mathbf{D}}_s\hat{\mathbf{E}}_s^H + \hat{\mathbf{E}}_n\hat{\mathbf{D}}_n\hat{\mathbf{E}}_n^H \tag{4}$$

where $\hat{\mathbf{D}}_s$ stands for a $K\times K$ diagonal matrix whose diagonal elements contain the K larger eigen-values and $\hat{\mathbf{D}}_n$ stands for a diagonal matrix whose diagonal entries contain the $3MN-K$ smaller eigen-values. $\hat{\mathbf{E}}_s$ is the matrix composed of the eigenvectors corresponding to the K larger eigen-values, while $\hat{\mathbf{E}}_n$ represents the matrix including the rest eigenvectors. Note that $\hat{\mathbf{E}}_s$ and $\hat{\mathbf{E}}_n$ can be regarded as the signal subspace and the noise subspace, respectively.

According to (1), the direction matrix is

$$\bar{\mathbf{A}} = \begin{bmatrix}\mathbf{A}\boldsymbol{\Phi}_x\\ \mathbf{A}\boldsymbol{\Phi}_y\\ \mathbf{A}\boldsymbol{\Phi}_z\end{bmatrix} \triangleq \begin{bmatrix}\mathbf{A}_1\\ \mathbf{A}_2\\ \mathbf{A}_3\end{bmatrix} \tag{5}$$

According to [23] and [24], the columns of the direction matrix span the same space as the signal subspace,

$$\hat{\mathbf{E}}_s = \bar{\mathbf{A}}\mathbf{T} \tag{6}$$

where $\mathbf{T}$ is a nonsingular unique full rank matrix.

The matrix $\hat{\mathbf{E}}_s$ can be partitioned as

$$\hat{\mathbf{E}}_s = \begin{bmatrix}\hat{\mathbf{E}}_1\\ \hat{\mathbf{E}}_2\\ \hat{\mathbf{E}}_3\end{bmatrix} = \begin{bmatrix}\mathbf{A}\boldsymbol{\Phi}_x\mathbf{T}\\ \mathbf{A}\boldsymbol{\Phi}_y\mathbf{T}\\ \mathbf{A}\boldsymbol{\Phi}_z\mathbf{T}\end{bmatrix} \tag{7}$$

According to (7), the follow matrix can be constructed

$$\begin{aligned}\hat{\mathbf{E}}_{xy} &= \hat{\mathbf{E}}_1 + j\hat{\mathbf{E}}_2\\ &= \mathbf{A}\boldsymbol{\Phi}_x\mathbf{T} + j\mathbf{A}\boldsymbol{\Phi}_y\mathbf{T}\\ &= \mathbf{A}\boldsymbol{\Phi}_{xy}\mathbf{T}\end{aligned} \tag{8}$$

where $\boldsymbol{\Phi}_{xy} = \boldsymbol{\Phi}_x + j\boldsymbol{\Phi}_y = \mathrm{diag}(\sin\theta_1 e^{j\phi_1},\ldots,\sin\theta_K e^{j\phi_K})$.

Then the rotational invariance between $\hat{\mathbf{E}}_3$ and $\hat{\mathbf{E}}_{xy}$ can be expressed as

$$\hat{\mathbf{E}}_3\boldsymbol{\Psi} = \hat{\mathbf{E}}_{xy} \tag{9}$$

where

$$\boldsymbol{\Psi} = \mathbf{T}^{-1}\boldsymbol{\Phi}_{xyz}\mathbf{T} \tag{10a}$$

and

$$\boldsymbol{\Phi}_{xyz} = \boldsymbol{\Phi}_z^{-1}\boldsymbol{\Phi}_{xy} = \mathrm{diag}\big(\tan\theta_1 e^{j\phi_1},\ldots,\tan\theta_K e^{j\phi_K}\big) \tag{10b}$$

From (10a), it can be shown that the diagonal elements of $\boldsymbol{\Phi}_{xyz}$ are the eigen-values of $\boldsymbol{\Psi}$. The least squares solution to Eq. (9) is

$$\hat{\boldsymbol{\Psi}} = \hat{\mathbf{E}}_3^{+}\hat{\mathbf{E}}_{xy} \tag{11}$$

Assume that the eigen-values of $\hat{\boldsymbol{\Psi}}$ are $\hat{z}_k$, $k=1,\ldots,K$, then according to (10), the elevation angle and azimuth angle can be estimated via

$$\hat{\theta}_k = \arctan\big(abs(\hat{z}_k)\big),\quad k=1,\ldots,K \tag{12a}$$

$$\hat{\phi}_k = angle(\hat{z}_k),\quad k=1,\ldots,K \tag{12b}$$

where $abs(\cdot)$ and $angle(\cdot)$ mean the taking amplitude and taking phase operations, respectively.

Remark 1. According to (7) and (9), the algorithm utilizes the rotational invariance ($\boldsymbol{\Phi}_x$, $\boldsymbol{\Phi}_y$ and $\boldsymbol{\Phi}_z$) between the three outputs of the velocity sensors, and the direction matrix $\mathbf{A}$ which contains the location information (2a)–(2b) of the sensors is not used. So the sensor location information is not required.

It should also be noted that the sensors locations can be unknown only when the geometric coordinate is already established, so the location of the reference point in Fig. 1 is needed actually. The reference point and the velocity sensor can determine the coordinate (see Fig. 1(a)). Thereafter, the sensors among the array can be arbitrarily located.

Remark 2. Automatically paired two-dimensional estimations of DOA can be obtained via the proposed algorithm. The estimated elevation angle and azimuth angle are corresponding to the same eigen-value of $\hat{\boldsymbol{\Psi}}$, so they are automatically paired.

Remark 3. According to (12), the elevation angle and azimuth angle that the proposed algorithm can estimate lie in the range [0 90] and [−180 180], respectively.

Remark 4. According to (7)–(9), the ESPRIT method we applied utilizes the relationship between the sub-arrays ($\hat{\mathbf{E}}_1$, $\hat{\mathbf{E}}_2$ and $\hat{\mathbf{E}}_3$; the length of the full subspace is $3MN$, and the length of the sub-array is MN), which leads to the array aperture loss. So there will be a gap between the proposed algorithm and CRB (see the simulation section). But the sensor location is unknown, so the information within the sub-arrays cannot be acquired.

Remark 5. In Eq. (4), the signal subspace $\hat{\mathbf{E}}_s$ can also be obtained by PM [19] with lower complexity, thereafter the angles can be estimated in the same way. However, it can be shown in the simulation section that the PM-based method will perform worse than the proposed method, especially in low signal to noise ratio (SNR).

The major steps of the proposed algorithm are shown as follows:

Step 1. Estimate the covariance matrix $\hat{\mathbf{R}}_x$ via

$$\hat{\mathbf{R}}_x = (1/J)\sum_{t=1}^{J}\mathbf{x}(t)\mathbf{x}^H(t)$$

Step 2. Perform eigen-decomposition operation for the covariance matrix to obtain $\hat{\mathbf{E}}_1, \hat{\mathbf{E}}_2$ and $\hat{\mathbf{E}}_3$ via (4) and (7).

Step 3. Obtain $\hat{\mathbf{E}}_{xy}$ via (8), and compute $\hat{\boldsymbol{\Psi}}$ via $\hat{\boldsymbol{\Psi}} = \hat{\mathbf{E}}_3^{+}\hat{\mathbf{E}}_{xy}$.

Step 4. Perform eigen-decomposition of $\hat{\mathbf{E}}_3^{+}\hat{\mathbf{E}}_{xy}$, and estimate the angles from the eigen-values via (12).

4. Error analysis

After the eigen-value decomposition, $\hat{\mathbf{R}}_x$ is denoted by

$$\hat{\mathbf{R}}_x = \hat{\mathbf{E}}\hat{\boldsymbol{\Lambda}}\hat{\mathbf{E}}^H \tag{13}$$

where $\hat{\mathbf{E}} = [\hat{\mathbf{S}}_1, \hat{\mathbf{S}}_2, \ldots, \hat{\mathbf{S}}_{3NM}]$ with $\hat{\mathbf{E}}$ being the estimated eigenvectors, and $\hat{\boldsymbol{\Lambda}} = \mathrm{diag}(\hat{\lambda}_1, \hat{\lambda}_2, \ldots, \hat{\lambda}_{3NM})$ with $\hat{\lambda}_i$ being the estimated eigen-value. Let $\hat{\mathbf{S}}_i = \mathbf{S}_i + \boldsymbol{\eta}_i$ and $\hat{\lambda}_i = \lambda_i + \xi_i$, then according to [25]

$$E\big[\boldsymbol{\eta}_i\boldsymbol{\eta}_j^H\big] \approx \frac{\lambda_i}{J}\sum_{\substack{l=1\\ l\neq i}}^{3NM}\frac{\lambda_l}{(\lambda_i-\lambda_l)^2}\mathbf{S}_l\mathbf{S}_l^H\delta_{ij},\quad i,j=1,\ldots,K \tag{14}$$

$$E\big[\boldsymbol{\eta}_i\boldsymbol{\eta}_j^T\big] \approx -\frac{\lambda_j\lambda_i}{J(\lambda_i-\lambda_j)^2}\mathbf{S}_j\mathbf{S}_i^T(1-\delta_{ij}),\quad i,j=1,\ldots,K \tag{15}$$

If z_i, $i=1,\ldots,K$, is the eigen-value of $\boldsymbol{\Psi}$, then the estimation error of z_i is

$$\Delta z_i = \mathbf{q}_i \Delta\boldsymbol{\Psi} \mathbf{x}_i \tag{16}$$

where $\mathbf{x}_i$ and $\mathbf{q}_i$ are the eigenvector and left eigenvector corresponding to z_i, respectively. $\boldsymbol{\Psi}\mathbf{x}_i = \mathbf{z}_i\mathbf{x}_i$, $\mathbf{q}_i\boldsymbol{\Psi} = \mathbf{z}_i\mathbf{q}_i$ and $\mathbf{q}_i\mathbf{x}_i = 1$.

As $(\mathbf{E}_3 + \Delta\mathbf{E}_3)(\boldsymbol{\Psi} + \Delta\boldsymbol{\Psi}) \approx \mathbf{E}_{xy} + \Delta\mathbf{E}_{xy}$, $\Delta\boldsymbol{\Psi}$ can be written approximately as

$$\Delta\boldsymbol{\Psi} \approx \mathbf{E}_3^+ \Delta\mathbf{E}_{xy} - \mathbf{E}_3^+ \Delta\mathbf{E}_3 \boldsymbol{\Psi} \tag{17}$$

According to (16) and (17), it can be shown that

$$\begin{aligned}\Delta z_i &= \mathbf{q}_i \mathbf{E}_3^+ [\Delta\mathbf{E}_{xy}\mathbf{x}_i - \Delta\mathbf{E}_3\boldsymbol{\Psi}\mathbf{x}_i] \\ &= \mathbf{q}_i \mathbf{E}_3^+ \left(\mathbf{W}' + j\mathbf{W}'' - z_i\mathbf{W}'''\right)\Delta\mathbf{E}_s\mathbf{x}_i\end{aligned} \tag{18}$$

where $\mathbf{W}' = [\mathbf{I}_{NM\times NM}, \mathbf{0}_{NM\times 2NM}]$, $\mathbf{W}'' = [\mathbf{0}_{NM\times NM}, \mathbf{I}_{NM\times NM}, \mathbf{0}_{NM\times NM}]$ and $\mathbf{W}''' = [\mathbf{0}_{NM\times NM}, \mathbf{0}_{NM\times NM}, \mathbf{I}_{NM\times NM}]$.

The mean squared error of z_i is given by

$$E\left[|\Delta z_i|^2\right] = \mathbf{q}_i \mathbf{E}_3^+ \mathbf{F}_i E\left[\Delta\mathbf{E}_s \mathbf{x}_i \mathbf{x}_i^H \Delta\mathbf{E}_s^H\right] \mathbf{F}_i^H \left(\mathbf{E}_3^+\right)^H \mathbf{q}_i^H \tag{19}$$

where $\mathbf{F}_i = \mathbf{W}' + j\mathbf{W}'' - z_i\mathbf{W}'''$.

Combine (14) and (19), then

$$\begin{aligned}&E\left[|\Delta z_i|^2\right] \\ &= \mathbf{q}_i \mathbf{E}_3^+ \left(\sum_{j=1}^{K} |\mathbf{x}_{ij}|^2 \mathbf{F}_i E\left[\boldsymbol{\eta}_j \boldsymbol{\eta}_j^H\right] \mathbf{F}_i^H\right) \left(\mathbf{q}_i \mathbf{E}_3^+\right)^H \\ &= \mathbf{q}_i \mathbf{E}_3^+ \mathbf{F}_i \left[\sum_{j=1}^{K} |\mathbf{x}_{ij}|^2 \frac{\lambda_j}{J} \sum_{\substack{k=1 \\ k\neq j}}^{3NM} \frac{\lambda_k}{(\lambda_j - \lambda_k)^2} \mathbf{S}_k \mathbf{S}_k^H\right] \mathbf{F}_i^H \left(\mathbf{q}_i \mathbf{E}_3^+\right)^H \\ &= \frac{1}{J} \mathbf{r}_i^H \left[\mathbf{x}_i^H \mathbf{W}_s \mathbf{x}_i \mathbf{E}_n \mathbf{E}_n^H + \mathbf{E}_s \mathbf{W} \mathbf{E}_s^H\right] \mathbf{r}_i \\ &= \frac{1}{J} \mathbf{r}_i^H \left[\mathbf{x}_i^H \mathbf{W}_s \mathbf{x}_i \mathbf{E}_n \mathbf{E}_n^H\right] \mathbf{r}_i \\ &= \frac{1}{J} \mathbf{r}_i^H \mathbf{r}_i \left[\bar{\mathbf{a}}_i^H \mathbf{E}_s \mathbf{W}_s \mathbf{E}_s^H \bar{\mathbf{a}}_i\right]\end{aligned} \tag{20}$$

where $\mathbf{W}_s \triangleq \operatorname{diag}\{\frac{\lambda_1\sigma^2}{(\lambda_1-\sigma^2)^2}, \ldots, \frac{\lambda_K\sigma^2}{(\lambda_K-\sigma^2)^2}\}$, $\mathbf{r}_i^H = (\mathbf{A}_3^+\mathbf{F}_i)^{(i)}$ denotes the ith row of $\mathbf{A}_3^+\mathbf{F}_i$, $\mathbf{A}_3^+ = (\mathbf{A}_3^H\mathbf{A}_3)^{-1}\mathbf{A}_3^H$ and $\bar{\mathbf{a}}_i$ is the ith column of $\bar{\mathbf{A}}$.

Similarly, we have

$$E\left[(\Delta z_i)^2\right] = \mathbf{r}_i^H \left(\sum_{j=1}^{K} \sum_{\substack{k=1 \\ k\neq j}}^{K} x_{ij} x_{ik} E\left[\boldsymbol{\eta}_j \boldsymbol{\eta}_k^T\right]\right) \mathbf{r}_i^* = 0 \tag{21}$$

The mean errors of θ_i and ϕ_i can be derived as follows

$$\begin{aligned}E\left[(\Delta\theta_i)^2\right] &= \frac{1}{2}\frac{\cos^4\theta_i}{\tan^2\theta_i}\left(E\left[\left|\Delta z_i z_i^*\right|^2\right] + \operatorname{Re}\left(E\left[\left(\Delta z_i z_i^*\right)^2\right]\right)\right) \\ &= \frac{\cos^4\theta_i}{2J} \mathbf{r}_i^H \mathbf{r}_i \left[\bar{\mathbf{a}}_i^H \mathbf{E}_s \mathbf{W}_s \mathbf{E}_s^H \bar{\mathbf{a}}_i\right]\end{aligned} \tag{22}$$

$$\begin{aligned}E\left[(\Delta\phi_i)^2\right] &= \frac{1}{2\tan^4\theta_i}\left(E\left[\left|\Delta z_i z_i^*\right|^2\right] - \operatorname{Re}\left(E\left[\left(\Delta z_i z_i^*\right)^2\right]\right)\right) \\ &= \frac{1}{2J\tan^2\theta_i} \mathbf{r}_i^H \mathbf{r}_i \left[\bar{\mathbf{a}}_i^H \mathbf{E}_s \mathbf{W}_s \mathbf{E}_s^H \bar{\mathbf{a}}_i\right]\end{aligned} \tag{23}$$

As $\cos^4\theta_i \leqslant \frac{1}{\tan^2\theta_i}$, then $E[(\Delta\theta_i)^2] \leqslant E[(\Delta\phi_i)^2]$, which means the mean error of the elevation is smaller than that of the azimuth angle (can also be shown in the simulation section).

The theoretical error and the simulation error will be compared in the simulation section, and it can be shown that they are almost the same.

5. CRB

In this section, we derive the CRB of DOA estimation in condition of the unknown sensor position in MIMO radar. The unknown parameters can be expressed as

$$\begin{aligned}\boldsymbol{\zeta} = \big[&\theta_1, \ldots, \theta_K, \phi_1, \ldots, \phi_K, x_{r1}, \ldots, x_{rN}, y_{r1}, \ldots, y_{rN}, \\ &z_{r1}, \ldots, z_{rN}, x_{t1}, \ldots, x_{tM}, y_{t1}, \ldots, y_{tM}, z_{t1}, \ldots, z_{tM}, \\ &\mathbf{b}_R^T(1), \ldots, \mathbf{b}_R^T(J), \mathbf{b}_I^T(1), \ldots, \mathbf{b}_I^T(J), \sigma^2\big]^T\end{aligned} \tag{24}$$

where $\mathbf{b}_R(j)$ and $\mathbf{b}_I(j)$ denote the real and imaginary parts of $\mathbf{b}(j)$, respectively.

The output with J snapshots is expressed as

$$\mathbf{y} = \left[\mathbf{x}^T(1), \ldots, \mathbf{x}^T(J)\right]$$

The mean $\boldsymbol{\mu}$ and the covariance matrix $\boldsymbol{\Gamma}$ of $\mathbf{y}$ are

$$\boldsymbol{\mu} = \begin{bmatrix} \bar{\mathbf{A}}\mathbf{b}(1) \\ \vdots \\ \bar{\mathbf{A}}\mathbf{b}(J) \end{bmatrix}, \qquad \boldsymbol{\Gamma} = \begin{bmatrix} \sigma^2\mathbf{I} & & 0 \\ & \ddots & \\ 0 & & \sigma^2\mathbf{I} \end{bmatrix} \tag{25}$$

From [26], the (i, j) element of the CRB matrix $(\mathbf{P}_{cr})$ is expressed as

$$\left[\mathbf{P}_{cr}^{-1}\right]_{ij} = \operatorname{tr}\left[\boldsymbol{\Gamma}^{-1}\boldsymbol{\Gamma}_i'\boldsymbol{\Gamma}^{-1}\boldsymbol{\Gamma}_j'\right] + 2\operatorname{Re}\left[\boldsymbol{\mu}_i'^*\boldsymbol{\Gamma}^{-1}\boldsymbol{\mu}_j'\right] \tag{26}$$

where $\boldsymbol{\Gamma}_i'$ and $\boldsymbol{\mu}_i'$ are the derivatives of $\boldsymbol{\Gamma}$ and $\boldsymbol{\mu}$ on the ith element of $\boldsymbol{\zeta}$, respectively. The covariance matrix is just related to σ^2, so the first part of (26) can be ignored. Then the (i, j) element of the CRB matrix $(\mathbf{P}_{cr})$ can be rewritten as

$$\left[\mathbf{P}_{cr}^{-1}\right]_{ij} = 2\operatorname{Re}\left[\boldsymbol{\mu}_i'^*\boldsymbol{\Gamma}^{-1}\boldsymbol{\mu}_j'\right] \tag{27}$$

Define $\mathbf{d}_{k\gamma} \triangleq \partial\bar{\mathbf{a}}_k/\partial\gamma_k$, $\gamma = \theta, \phi$, then according to (25),

$$\frac{\partial\boldsymbol{\mu}}{\partial\gamma_k} = \begin{bmatrix} \mathbf{d}_{k\gamma}\mathbf{b}_k(1) \\ \vdots \\ \mathbf{d}_{k\gamma}\mathbf{b}_k(J) \end{bmatrix}, \quad k = 1, \ldots, K, \ \gamma = \theta, \phi \tag{28}$$

where $\mathbf{b}_k(t)$ is the kth element of $\mathbf{b}(t)$. And define $\mathbf{D}_\rho \triangleq \partial\bar{\mathbf{A}}/\partial\rho$, $\rho = x_{rn}, y_{rn}, z_{rn}, x_{tm}, y_{tm}, z_{tm}$, then

$$\begin{aligned}\frac{\partial\boldsymbol{\mu}}{\partial\rho} &= \begin{bmatrix} \mathbf{D}_\rho\mathbf{b}(1) \\ \vdots \\ \mathbf{D}_\rho\mathbf{b}(J) \end{bmatrix} \\ k &= 1, \ldots, K, \ \rho = x_{rn}, y_{rn}, z_{rn}, x_{tm}, y_{tm}, z_{tm}\end{aligned} \tag{29}$$

Let

$$\boldsymbol{\Delta}_1 \triangleq \begin{bmatrix} \mathbf{d}_{1\theta}\mathbf{b}_1(1) & \cdots & \mathbf{d}_{K\theta}\mathbf{b}_K(1) & \mathbf{d}_{1\phi}\mathbf{b}_1(1) & \cdots & \mathbf{d}_{K\phi}\mathbf{b}_K(1) \\ \vdots & & \vdots & \vdots & & \vdots \\ \mathbf{d}_{1\theta}\mathbf{b}_1(J) & \cdots & \mathbf{d}_{K\theta}\mathbf{b}_K(J) & \mathbf{d}_{1\phi}\mathbf{b}_1(J) & \cdots & \mathbf{d}_{K\phi}\mathbf{b}_K(J) \end{bmatrix} \tag{30}$$

$$\boldsymbol{\Delta}_2 \triangleq \begin{bmatrix} \mathbf{D}_{xr1}\mathbf{b}(1) & \cdots & \mathbf{D}_{xrN}\mathbf{b}(1) & \mathbf{D}_{yr1}\mathbf{b}(1) & \cdots & \mathbf{D}_{yrN}\mathbf{b}(1) & \mathbf{D}_{zr1}\mathbf{b}(1) & \cdots & \mathbf{D}_{zrN}\mathbf{b}(1) \\ \vdots & & \vdots & \vdots & & \vdots & \vdots & & \vdots \\ \mathbf{D}_{xr1}\mathbf{b}(J) & \cdots & \mathbf{D}_{xrN}\mathbf{b}(J) & \mathbf{D}_{yr1}\mathbf{b}(J) & \cdots & \mathbf{D}_{yrN}\mathbf{b}(J) & \mathbf{D}_{zr1}\mathbf{b}(J) & \cdots & \mathbf{D}_{zrN}\mathbf{b}(J) \end{bmatrix} \tag{31}$$

$$\boldsymbol{\Delta}_3 \triangleq \begin{bmatrix} \mathbf{D}_{xt1}\mathbf{b}(1) & \cdots & \mathbf{D}_{xtM}\mathbf{b}(1) & \mathbf{D}_{yt1}\mathbf{b}(1) & \cdots & \mathbf{D}_{ytM}\mathbf{b}(1) & \mathbf{D}_{zt1}\mathbf{b}(1) & \cdots & \mathbf{D}_{ztM}\mathbf{b}(1) \\ \vdots & & \vdots & \vdots & & \vdots & \vdots & & \vdots \\ \mathbf{D}_{xt1}\mathbf{b}(J) & \cdots & \mathbf{D}_{xtM}\mathbf{b}(J) & \mathbf{D}_{yt1}\mathbf{b}(J) & \cdots & \mathbf{D}_{ytM}\mathbf{b}(J) & \mathbf{D}_{zt1}\mathbf{b}(J) & \cdots & \mathbf{D}_{ztM}\mathbf{b}(J) \end{bmatrix} \tag{32}$$

And let

$$\mathbf{G} \triangleq \begin{bmatrix} \bar{\mathbf{A}} & & 0 \\ & \ddots & \\ 0 & & \bar{\mathbf{A}} \end{bmatrix}, \qquad \mathbf{b} = \begin{bmatrix} \mathbf{b}(1) \\ \vdots \\ \mathbf{b}(J) \end{bmatrix} \tag{33}$$

As $\boldsymbol{\mu} = \mathbf{G}\mathbf{b}$, then

$$\frac{\partial \boldsymbol{\mu}}{\partial \mathbf{b}_R^T} = \mathbf{G}, \qquad \frac{\partial \boldsymbol{\mu}}{\partial \mathbf{b}_I^T} = j\mathbf{G} \tag{34}$$

Now it can be written that

$$\frac{\partial \boldsymbol{\mu}}{\partial \boldsymbol{\zeta}^T} = [\boldsymbol{\Delta}_1, \boldsymbol{\Delta}_2, \boldsymbol{\Delta}_3, \mathbf{G}, j\mathbf{G}, 0] \tag{35}$$

Define $\boldsymbol{\Delta} = [\boldsymbol{\Delta}_1, \boldsymbol{\Delta}_2, \boldsymbol{\Delta}_3]$, then Eq. (27) can be denoted by

$$2\,\mathrm{Re}\left\{ \frac{\partial \boldsymbol{\mu}^*}{\partial \boldsymbol{\zeta}} \boldsymbol{\Gamma}^{-1} \frac{\partial \boldsymbol{\mu}}{\partial \boldsymbol{\zeta}^T} \right\} = \begin{bmatrix} \mathbf{J} & 0 \\ 0 & 0 \end{bmatrix} \tag{36}$$

where

$$\mathbf{J} \triangleq \frac{2}{\sigma^2}\,\mathrm{Re}\left\{ \begin{bmatrix} \boldsymbol{\Delta}^H \\ \mathbf{G}^H \\ -j\mathbf{G}^H \end{bmatrix} [\,\boldsymbol{\Delta} \quad \mathbf{G} \quad j\mathbf{G}\,] \right\}$$

As we can just consider the elements related to the angles in $\mathbf{J}^{-1}$, define

$$\mathbf{B} \triangleq \left(\mathbf{G}^H\mathbf{G}\right)^{-1}\mathbf{G}^H\boldsymbol{\Delta} \tag{37}$$

$$\mathbf{F} \triangleq \begin{bmatrix} \mathbf{I} & 0 & 0 \\ -\mathbf{B}_R & \mathbf{I} & 0 \\ -\mathbf{B}_I & 0 & \mathbf{I} \end{bmatrix} \tag{38}$$

It can be demonstrated that

$$[\,\boldsymbol{\Delta} \quad \mathbf{G} \quad j\mathbf{G}\,]\mathbf{F} = \left[\,(\boldsymbol{\Delta} - \mathbf{G}\mathbf{B}) \quad \mathbf{G} \quad j\mathbf{G}\right] = \left[\,\boldsymbol{\Pi}_{\mathbf{G}}^{\perp}\boldsymbol{\Delta} \quad \mathbf{G} \quad j\mathbf{G}\right] \tag{39}$$

where $\boldsymbol{\Pi}_{\mathbf{G}}^{\perp} = \mathbf{I} - \mathbf{G}(\mathbf{G}^H\mathbf{G})^{-1}\mathbf{G}^H$ and $\mathbf{G}^H\boldsymbol{\Pi}_{\mathbf{G}}^{\perp} = 0$.

$$\begin{aligned} \mathbf{F}^T\mathbf{J}\mathbf{F} &= \frac{2}{\sigma^2}\,\mathrm{Re}\left\{ \mathbf{F}^H \begin{bmatrix} \boldsymbol{\Delta}^H \\ \mathbf{G}^H \\ -j\mathbf{G}^H \end{bmatrix} [\,\boldsymbol{\Delta} \quad \mathbf{G} \quad j\mathbf{G}\,]\mathbf{F} \right\} \\ &= \frac{2}{\sigma^2}\,\mathrm{Re}\left\{ \begin{bmatrix} \boldsymbol{\Delta}^H\boldsymbol{\Pi}_{\mathbf{G}}^{\perp} \\ \mathbf{G}^H \\ -j\mathbf{G}^H \end{bmatrix} [\,\boldsymbol{\Pi}_{\mathbf{G}}^{\perp}\boldsymbol{\Delta} \quad \mathbf{G} \quad j\mathbf{G}\,] \right\} \\ &= \frac{2}{\sigma^2}\,\mathrm{Re}\left\{ \begin{bmatrix} \boldsymbol{\Delta}^H\boldsymbol{\Pi}_{\mathbf{G}}^{\perp}\boldsymbol{\Delta} & 0 & 0 \\ 0 & \mathbf{G}^H\mathbf{G} & j\mathbf{G}^H\mathbf{G} \\ 0 & -j\mathbf{G}^H\mathbf{G} & \mathbf{G}^H\mathbf{G} \end{bmatrix} \right\} \end{aligned} \tag{40}$$

So $\mathbf{J}^{-1}$ is written as

$$\begin{aligned} \mathbf{J}^{-1} &= \mathbf{F}\left(\mathbf{F}^T\mathbf{J}\mathbf{F}\right)^{-1}\mathbf{F}^T \\ &= \frac{\sigma^2}{2} \begin{bmatrix} \mathbf{I} & 0 & 0 \\ -\mathbf{B}_R & \mathbf{I} & 0 \\ -\mathbf{B}_I & 0 & \mathbf{I} \end{bmatrix} \begin{bmatrix} \mathrm{Re}(\boldsymbol{\Delta}^H\boldsymbol{\Pi}_{\mathbf{G}}^{\perp}\boldsymbol{\Delta}) & 0 & 0 \\ 0 & \kappa & \kappa \\ 0 & \kappa & \kappa \end{bmatrix} \\ &\quad \times \begin{bmatrix} \mathbf{I} & -\mathbf{B}_R^T & -\mathbf{B}_I^T \\ 0 & \mathbf{I} & 0 \\ 0 & 0 & \mathbf{I} \end{bmatrix} \\ &= \begin{bmatrix} \frac{\sigma^2}{2}[\mathrm{Re}(\boldsymbol{\Delta}^H\boldsymbol{\Pi}_{\mathbf{G}}^{\perp}\boldsymbol{\Delta})]^{-1} & \kappa & \kappa \\ & \kappa & \kappa \\ & \kappa & \kappa \end{bmatrix} \end{aligned}$$

where κ denotes the redundant part. Till now, the CRB matrix can be given as follows

$$CRB = \frac{\sigma^2}{2}\left[\mathrm{Re}\left(\boldsymbol{\Delta}^H\boldsymbol{\Pi}_{\mathbf{G}}^{\perp}\boldsymbol{\Delta}\right)\right]^{-1} \tag{41}$$

The first $2K$ elements of the CRB matrix will be the bound of the mean square error of the angles, and it will be utilized in the simulation to compare with the algorithms to measure their angle estimation performances.

6. Complexity analysis

The computational complexity can be measured by the times of the complex multiplication. In the proposed method, the estimation of the covariance matrix needs $O(JM^2N^2)$, the eigen-decomposition to obtain the signal subspace costs $O(M^3N^3)$, the pseudo-inverse operation requires $O(K^2MN)$ and the final eigen-decomposition and angle estimation cost $O(K^3)$. The proposed algorithm has low complexity for it requires no peak search, which is necessary in the MUSIC-like algorithms [7,8,24]. PM [19] can also be applied for the angle estimation in this paper, and it will reduce the complexity when calculate the signal subspace. PM requires about $O(M^2N^2K)$ to obtain the signal subspace, and has the same complexity with the proposed in other steps. So PM will have slightly lower complexity, but it has worse performance than the proposed algorithm, especially in low SNR (see the simulation section).

The proposed algorithm has the following advantages.

(1) It can be suitable for arbitrary array.
(2) It can obtain automatically paired two-dimensional angle estimations.
(3) It has low complexity, since it requires no peak searching.
(4) It requires no knowledge of the location of the sensors in the array.

7. Simulation results

Monte Carlo simulations are presented to assess the angle estimation performance of the proposed algorithm. Define root mean squared error (RMSE) as

$$\frac{1}{K}\sum_{k=1}^{K}\sqrt{\frac{1}{1000}\sum_{l=1}^{1000}\left[(\hat{\theta}_{k,l}-\theta_k)^2 + (\hat{\phi}_{k,l}-\phi_k)^2\right]}$$

where $\hat{\theta}_{k,l}$ and $\hat{\phi}_{k,l}$ are the estimates of elevation and azimuth of the lth Monte Carlo trial, respectively. In the following simulations, we normally adopt the monostatic MIMO array system with $M = 8$ and $N = 8$, and assume that there are two non-coherent targets located at angles $(\theta_1, \phi_1) = (10^\circ, 15^\circ)$ and $(\theta_2, \phi_2) = (20^\circ, 25^\circ)$, respectively.

Figs. 2–3 present the angle estimation results of the proposed algorithm for all two targets with $J = 100$ and different SNR, where elevation and azimuth can be clearly observed, and the estimation performance improves as the SNR increases. It can also be shown that the estimations along the azimuth have greater deviation, which has been proved in the error analysis section.

Figs. 4–5 show the elevation and azimuth estimation performance comparison, where we compare the proposed algorithm with PM [19], theoretical RMSE of the proposed and CRB

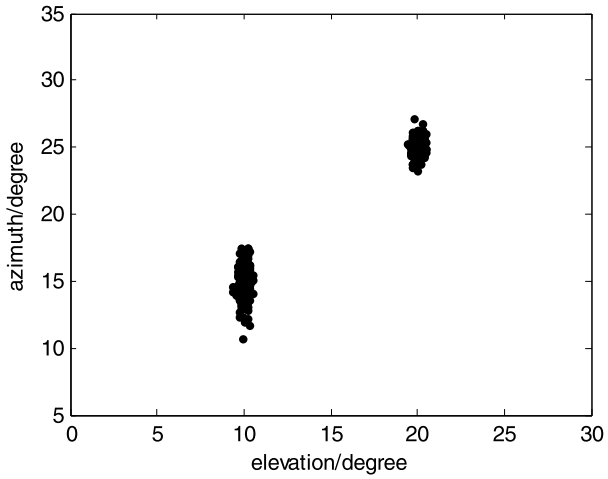

Fig. 2. Angle estimation results with SNR = 15 dB.

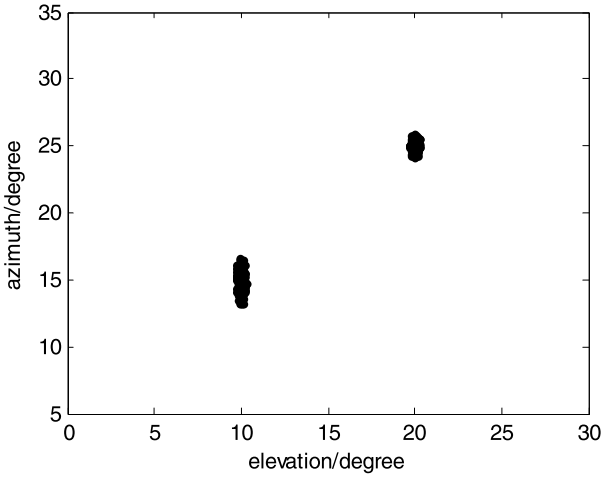

Fig. 3. Angle estimation results with SNR = 20 dB.

(derived in Section 5). From Figs. 4–5, we can find that the proposed algorithm has better angle estimation performance than PM, especially in low SNR. The theoretical error and simulation error of the proposed algorithm are almost the same, which demonstrates the correctness of the derivation in Section 4.

Fig. 6 depicts the algorithmic performance with different J ($M = N = 8$). It is indicated that the performance of angle estimation for MIMO array becomes better in collaboration with J increasing. According to Eqs. (14)–(15), the increase of J will reduce the estimation error of the signal subspace, which will lead to the performance improvement.

Figs. 7–8 illustrate the elevation and azimuth estimation performances of the proposed algorithm with different number of transmit and receive antennas, respectively. It is clearly shown that the angle estimation performance of the proposed algorithm is gradually improved with the number of antennas increasing. Multiple antennas improve DOA estimation performance because of diversity gain.

In Figs. 9–10, the estimation results of the proposed algorithm with the same elevation angle and the same azimuth angle are tested, respectively. The angles are (1) $(\theta_1, \phi_1) = (20°, 15°)$, $(\theta_2, \phi_2) = (20°, 25°)$ and (2) $(\theta_1, \phi_1) = (10°, 25°)$, $(\theta_2, \phi_2) = (20°, 25°)$, respectively. It can be shown that the proposed algorithm can work well when the targets have the same elevation angle or the same azimuth angle.

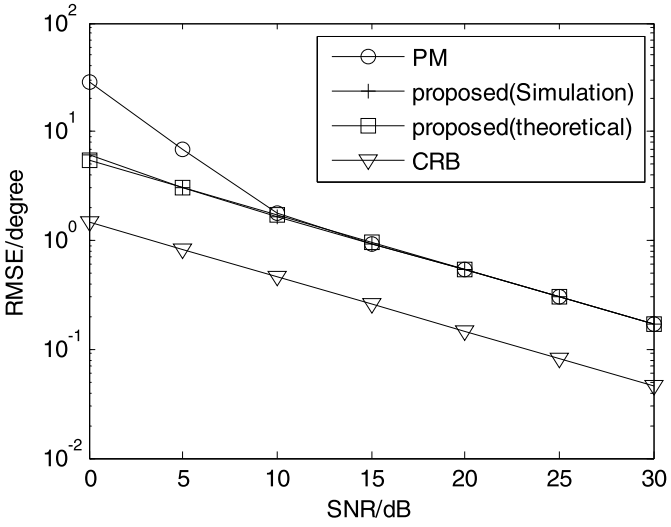

Fig. 4. Angle estimation performance comparison ($M = 8$, $N = 8$, $J = 100$).

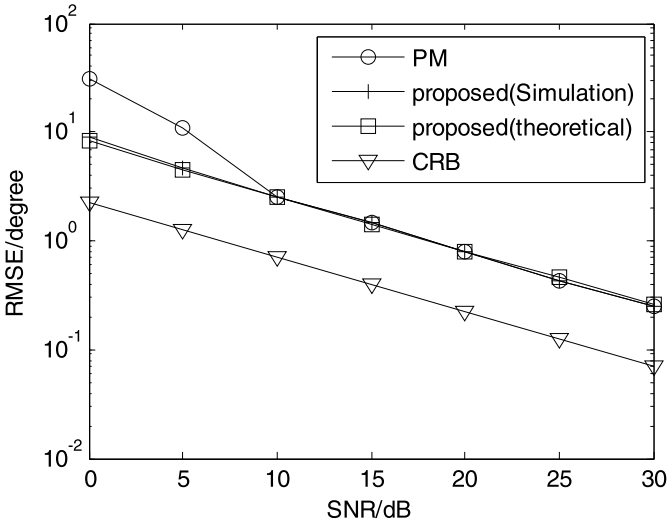

Fig. 5. Angle estimation performance comparison ($M = 8$, $N = 6$, $J = 50$).

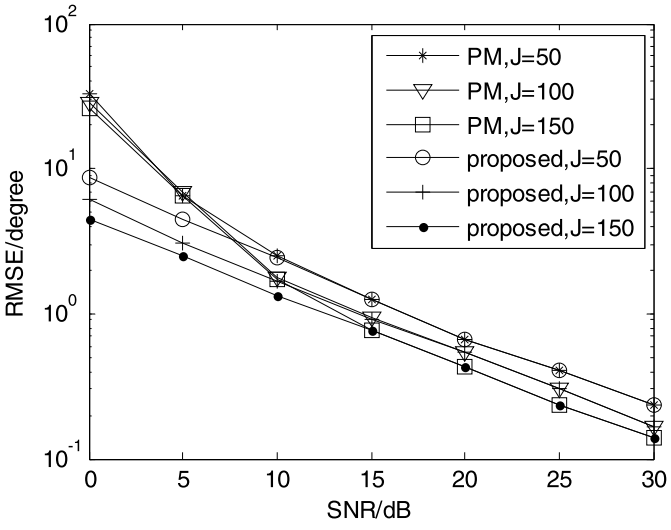

Fig. 6. Angle estimation performance with different values of J.

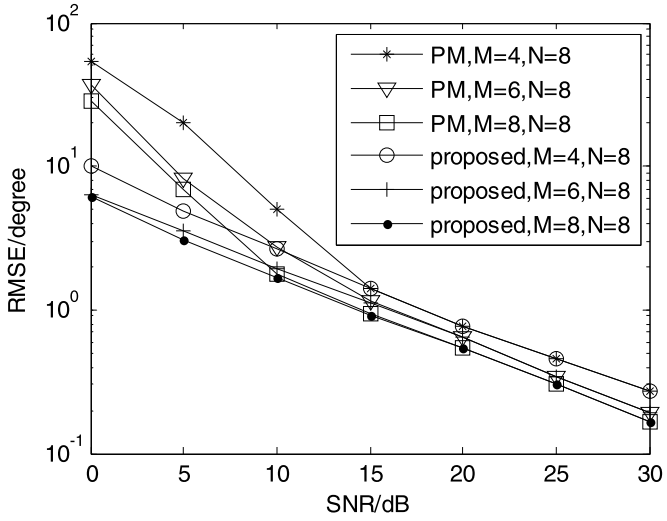

Fig. 7. Angle estimation performance with different number of transmit antennas.

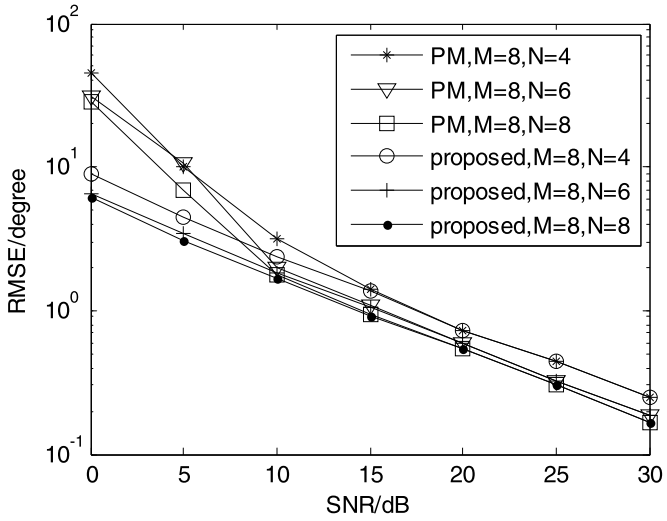

Fig. 8. Angle estimation performance with different number of receive antennas.

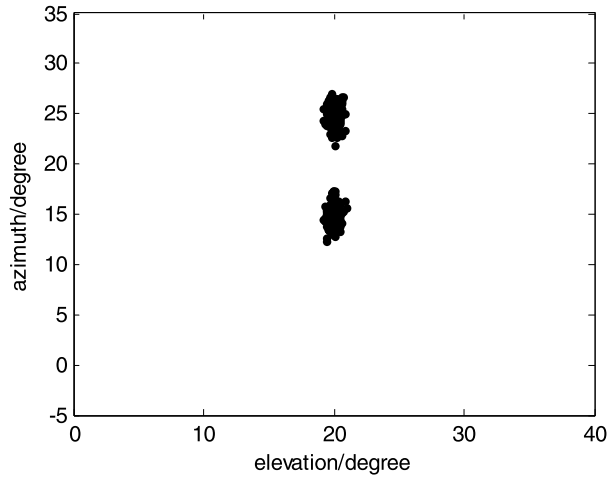

Fig. 9. Angle estimation results with the same elevation angle (SNR = 20 dB).

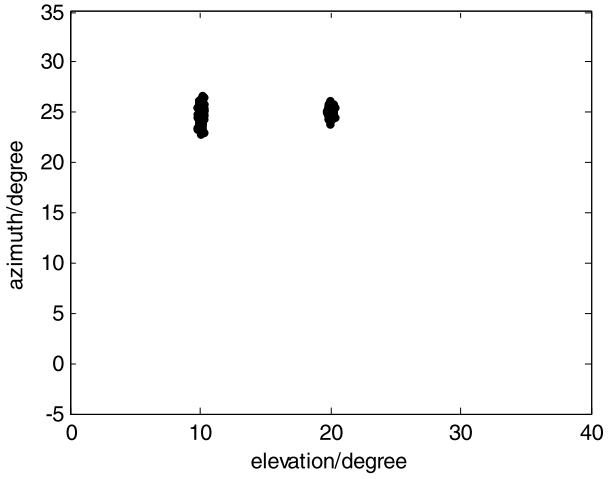

Fig. 10. Angle estimation results with the same azimuth angle (SNR = 20 dB).

8. Conclusions

In this paper, we have proposed an algorithm based on ESPRIT for angle estimation in monostatic MIMO array with velocity receive sensors. The algorithm imposes no constraint on the array geometry and the location of the sensors due to the characteristics of the outputs of velocity sensors. According to the relationship between the outputs along different axis, ESPRIT can be employed to estimate the angles accurately regardless of the detail outputs along the axis. The proposed algorithm has very low complexity and requires no pair matching. Furthermore, it has better angle estimation performance than the propagator method using on the same sensor configuration. Additionally, the error analysis of the angle estimation, the complexity analysis and CRB have been derived to analyze the performance.

Acknowledgments

This work is supported by China NSF Grants (61201208, 61271327, 61071164), Jiangsu Planned Projects for Postdoctoral Research Funds (1201039C), China Postdoctoral Science Foundation (2012M521099), Open Project of Key Laboratory of Underwater Acoustic Communication and Marine Information Technology (Xiamen University), Hubei Key Laboratory of Intelligent Wireless Communications (IWC2012002), Open Project of Key Laboratory of Nondestructive Testing (Nanchang Hangkong University), Open Project of Key Laboratory of Modern Acoustic of Ministry of Education (Nanjing University), the Aeronautical Science Foundation of China (20120152001), Research Innovation Program for College Graduates of Jiangsu Province (CXZZ13_0165), Funding for Outstanding Doctoral Dissertation in NUAA (BCXJ13-09), by Qing Lan Project, PAPD of Jiangsu Higher Education Institutions and the Fundamental Research Funds for the Central Universities (NS2013024, NZ2012010, kfjj120115, kfjj20110215).

References

[1] E. Fishler, A. Haimovich, R.S. Blum, L.J. Cimini, D. Chizhik, R.A. Valenzuela, MIMO radar: An idea whose time has come, in: Proc. IEEE Radar Conf., Apr. 2004, pp. 71–78.
[2] J. Li, P. Stoica, MIMO radar—Diversity means superiority, in: Proc. 14th Adaptive Sensor Array Process. Workshop (ASAP'06), Lincoln Lab, MA, USA, Dec. 2006.
[3] J. Li, P. Stoica, L. Xu, W. Roberts, On parameter identifiability of MIMO radar, IEEE Signal Process. Lett. 14 (12) (Dec. 2007) 968–971.
[4] L. Xu, J. Li, P. Stoica, Target detection and parameter estimation for MIMO radar systems, IEEE Trans. Aerosp. Electron. Syst. 44 (3) (Jul. 2008) 927–939.
[5] J. Zhang, L. Zhang, N. Liu, Maximal likelihood DOA estimation of MIMO radar, Syst. Eng. Electron. 31 (6) (Jun. 2009) 1292–1294.

[6] H. Yan, J. Li, G. Liao, Multitarget identification and localization using bistatic MIMO radar systems, EURASIP J. Adv. Signal Process. (2008) 1–8, Article ID283483.
[7] X. Gao, X. Zhang, G. Feng, et al., On the MUSIC-derived approaches of angle estimation for bistatic MIMO radar, in: WNIS'09. International Conference on Wireless Networks and Information Systems, Dec. 2009, pp. 343–346.
[8] X. Zhang, L. Xu, L. Xu, et al., Direction of Departure (DOD) and Direction of Arrival (DOA) estimation in MIMO radar with reduced-dimension MUSIC, IEEE Commun. Lett. 14 (12) (Dec. 2010) 1161–1163.
[9] R. Xie, Z. Liu, J. Wu, Direction finding with automatic pairing for bistatic MIMO radar, Signal Process. 92 (1) (Jan. 2012) 198–203.
[10] R. Roy, T. Kailath, ESPRIT-estimation of signal parameters via rotational invariance techniques, IEEE Trans. Acoust. Speech Signal Process. 37 (1989) 984–995.
[11] C. Duofang, C. Baixiao, Q. Guodong, Angle estimation using ESPRIT in MIMO radar, Electron. Lett. 44 (12) (Jun. 2008) 770–771.
[12] C. Jinli, G. Hong, S. Weimin, Angle estimation using ESPRIT without pairing in MIMO radar, Electron. Lett. 44 (24) (Nov. 2008) 1422–1423.
[13] M. Jin, G. Liao, J. Li, Joint DOD and DOA estimation for bistatic MIMO radar, Signal Process. 89 (2) (2009) 244–251.
[14] G. Zheng, B. Chen, M. Yang, Unitary ESPRIT algorithm for bistatic MIMO radar, Electron. Lett. 48 (3) (Feb. 2012) 179–181.
[15] X. Zhang, D. Xu, Low-complexity ESPRIT-based DOA estimation for collocated MIMO radar using reduced-dimension transformation, Electron. Lett. 47 (4) (2011) 283–284.
[16] C. Li, G. Liao, S. Zhu, S. Wu, An ESPRIT-like algorithm for coherent DOA estimation based on data matrix decomposition in MIMO radar, Signal Process. 91 (8) (Aug. 2011) 1803–1811.
[17] S. Marcos, A. Marsal, M. Benidir, The propagator method for source bearing estimation, Signal Process. 42 (1995) 121–138.
[18] J. Chen, H. Gu, W. Su, A method for fast multi-targets location in bistatic MIMO-radar system, J. Electron. Inform. Technol. 31 (7) (2009) 1664–1668.
[19] Z.D. Zheng, J.Y. Zhang, Fast method for multi-target localization in bistatic MIMO radar, Electron. Lett. 47 (2) (2011) 138–139.
[20] X. Zhang, Z. Xu, L. Xu, D. Xu, Trilinear decomposition-based transmit angle and receive angle estimation for multiple-input multiple-output radar, IET Radar Sonar Navig. 5 (6) (Jul. 2011) 626–631.
[21] J. Li, X. Zhang, Closed-form blind 2D-DOD and 2D-DOA estimation for MIMO radar with arbitrary arrays, Wirel. Pers. Commun. (Mar. 2012) 1–12, http://dx.doi.org/10.1007/s11277-012-0567-9.
[22] A. Nehorai, E. Paldi, Acoustic vector-sensor array processing, IEEE Trans. Signal Process. 42 (9) (Sept. 1994) 2481–2491.
[23] K.T. Wong, M.D. Zoltowski, Closed-form underwater acoustic direction-finding with arbitrarily spaced vector hydrophones at unknown locations, IEEE J. Ocean. Eng. 22 (3) (Jul. 1997) 566–575.
[24] J. He, M.N.S. Swamy, M. Omair Ahmad, Joint DOD and DOA estimation for MIMO array with velocity receive sensors, IEEE Signal Process. Lett. 18 (7) (Jul. 2011) 399–402.
[25] B.D. Rao, K.V.S. Hari, Performance analysis of ESPRIT and TAM in determining the direction of arrival of plane waves in noise, IEEE Trans. Acoust. Speech Signal Process. 40 (12) (1989) 1990–1995.
[26] P. Stoica, A. Nehorai, Performance study of conditional and unconditional direction-of-arrival estimation, IEEE Trans. Signal Process. 38 (10) (Oct. 1990) 1783–1795.

Jianfeng Li now is a doctoral student in Department of Electronic Engineering, Nanjing University of Aeronautics & Astronautics. His research is focused on array signal processing and communication signal processing.

Xiaofei Zhang received M.S degree in electrical engineering from Wuhan University, Wuhan, China, in 2001. He received Ph.D. degrees in communication and information systems from Nanjing University of Aeronautics and Astronautics in 2005. Now, he is a Professor in Electronic Engineering Department, Nanjing University of Aeronautics & Astronautics, Nanjing, China. His research is focused on array signal processing and communication signal processing.